ISSN 1069-3513, Izvestiya, Physics of the Solid Earth, 2014, Vol. 50, No. 2, pp. 249–262. © Pleiades Publishing, Ltd., 2014.
Original Russian Text © A.A. Shlykov, A.K. Saraev, 2014, published in Fizika Zemli, 2014, No. 2, pp. 258–271.

# Wave Effects in the Field of a High-Frequency Horizontal Electric Dipole

**A. A. Shlykov and A. K. Saraev**

*St. Petersburg State University, Faculty of Geology, Universitetskaya nab., 7/9, St. Petersburg, 199034 Russia*

*e-mail: shlykovarseny@gmail.com*

Received May 22, 2013; in final form, October 5, 2013

**Abstract**—A normal electromagnetic field of the high-frequency horizontal electric dipole is analyzed with allowance for the displacement currents in the earth and air. The components of the field are calculated by the method of partial integration for nonsmooth behavior of the integrand. The boundary between the quasi-stationary and wave zone of the source is established according to the results of calculations. The effects arising in the wave zone due to the displacement currents in the air are considered. The results of the calculations are confirmed by field experiments.

*Keywords*: high-frequency horizontal electric dipole, displacement current, wave zone

**DOI:** 10.1134/S1069351314020104

## INTRODUCTION

The low-frequency electromagnetic prospecting methods such as magnetotelluric sounding (MT), frequency sounding (FS), and controlled-source audiomagnetotelluric (CSAMT) sounding have recently become widely popular. These methods typically use frequencies ranging from a few ten-thousandth fractions of a Hz to a few dozens of kHz and are focused on studying the section at large depths spanning from dozens of meters to dozens of kilometers. The physical background of these methods relies on the quasi-stationary model of the electromagnetic (EM) field. Impedance measurements (the ratio of the horizontal and mutually orthogonal components of the electrical and magnetic fields) in the far-field zone of the sources, either natural or controlled, make it possible to eliminate the effects of the instability of the sources in the results of the sounding. The well-developed methods and software tools for interpretation of their measurements provide reliable information on the depth distribution of electrical resistivity in laterally homogeneous and heterogeneous media (Berdichevsky and Dmitriev, 2009; deGroot-Hedlin and Constable, 1990; Smith and Booker, 1991, et al.).

Recently, EM sounding methods with high frequency (HF) EM fields (varying from a few thousand kHz to dozens of MHz) have been rapidly advancing. These methods are applied to study shallow sections spanning from 1–2 m to dozens of meters (Bastani, 2001; Song, Kim, and Lee, 2002; Tezkan and Saraev, 2008; Kalscheuer, Pedersen, and Siripunvaraporn, 2008; Simakov et al., 2010; Khmelevskoi et al., 2010; Saraev et al., 2011). The HF methods employ the EM fields from broadcasting radio transmitters or their own controlled sources. The data provided by these methods allow us to estimate the electrical resistivity and dielectric permittivity of the rocks, which enhances the informativity of the soundings and expands the range of the solved problems. At the same time, in the case of HF soundings, the displacement currents in the earth and air affect the behavior of the components of the EM field, and these effects should be taken into account.

Previously, the analysis of the influence of the displacement currents in the earth and air on the EM field components was focused on assessing the applicability of the quasi-stationary approximation for the fields generated by controlled sources and the possibility to estimate the permittivity of the rocks (Veshev, Ladatko, and Morozova, 1983; Egorova and Sapozhnikov, 1983; Yin and Hodges, 2005; Siemon, 2012). The present paper addresses the study of the structure of the normal (above the half-space) EM field of a HF horizontal electric dipole (HED) used as the source in a series of HF EM methods, including the controlled-source radio magnetotelluric (RMT) sounding (Simakov et al., 2010; Saraev et al., 2011).

## QUASI-STATIONARY APPROXIMATION

The calculations and analysis of the EM field generated by HED are discussed by many Russian (Fock, 1933; Zaborovskii, 1960; Veshev, 1980; Vanyan, 1997, etc.) and foreign (Stefanescu, 1950; Ward and Hohmann, 1987, etc.) authors. In these studies, the quasi-stationary field generated by HED is mainly consid-

ered in the application to the low-frequency electromagnetic prospecting method.

The components of the EM field generated by HED with moment $\beta = Idl\mu_0/4\pi$, which is located on the surface of a homogeneous half-space (the normal field) and oriented along the $x$ axis (the $z$ axis points vertically upwards) with the time dependence described by $e^{+i\omega t}$ have the following form (Veshev, 1980):

$$E_x^{(1)} = \frac{Idl}{2\pi} i\omega\mu_0 \left[ \frac{\partial^2}{\partial x^2} \int_0^\infty \frac{m e^{n_1 z}}{k_0^2 n_1 + k_1^2 n_0} J_0(mr)dm - \int_0^\infty \frac{m e^{n_1 z}}{n_0 + n_1} J_0(mr)dm \right],$$

$$E_y^{(1)} = \frac{Idl}{2\pi} i\omega\mu_0 \frac{\partial^2}{\partial x \partial y} \int_0^\infty \frac{m e^{n_1 z}}{k_0^2 n_1 + k_1^2 n_0} J_0(mr)dm,$$

$$H_x^{(0)} = \frac{Idl}{2\pi}(k_1^2 - k_0^2) \times \frac{\partial^2}{\partial x \partial y} \int_0^\infty \frac{m e^{-n_0 z}}{(n_0 + n_1)(k_0^2 n_1 + k_1^2 n_0)} J_0(mr)dm, \quad (1)$$

$$H_y^{(0)} = -\frac{Idl}{2\pi} \left[ \int_0^\infty \frac{n_0 m e^{-n_0 z}}{n_0 + n_1} J_0(mr)dm + (k_1^2 - k_0^2) \frac{\partial^2}{\partial x^2} \int_0^\infty \frac{m e^{-n_0 z}}{(n_0 + n_1)(k_0^2 n_1 + k_1^2 n_0)} J_0(mr)dm \right],$$

$$H_z^{(0)} = -\frac{Idl}{2\pi} \frac{\partial}{\partial y} \int_0^\infty \frac{m e^{-n_0 z}}{n_0 + n_1} J_0(mr)dm.$$

Here, $I$ is the current strength, A; $dl$ is the length of the dipole, m; $i$ is the imaginary unity; $\omega = 2\pi f$ is angular frequency; $f$ is frequency, Hz; $k_j^2 = i\omega\mu_0(\sigma_j + i\omega\varepsilon_j)$ is the squared wave number in the $j$th layer; $n_j = \sqrt{k_j^2 + m^2}$; $\sigma_j$ is the electrical conductivity, S/m; $\varepsilon_j$ is absolute permittivity ($\varepsilon_j = \varepsilon_j^{\text{rel}} \times 10^{-9}/36\pi$, F/m, where $\varepsilon_j^{\text{rel}}$ is the relative permittivity); $j = 0,1$; $r = \sqrt{x^2 + y^2}$, m; $J_0$ is the zero-order Bessel function of the first kind.

The formulas for electrical components are presented for medium 1 (in the ground), and for magnetic components, for medium 0 (in the air). The weak-magnetic media are considered, and the magnetic permeability of the earth and air is assumed to be equal to the permeability of free space: $\mu_1 = \mu_0 = 4\pi \times 10^{-7}$ H/m.

Within the quasi-stationary approximation, with the observation point located on the earth's surface ($z = 0$), at rather low frequencies, and with the assumptions that $k_0 = 0$ and $k_1 = \sqrt{i\omega\mu_0\sigma_1}$, formulas (1) are converted by the approaches suggested by V.A. Fock (1933) to the following form (Veshev, 1980):

$$E_x^{(1)} = \frac{Idl\rho_1}{2\pi r^3}\left[3\cos^2\theta + (1 + k_1 r)e^{-k_1 r} - 2\right],$$

$$E_y^{(1)} = \frac{3Idl\rho_1}{4\pi r^3}\sin 2\theta,$$

$$H_x^{(0)} = \frac{Idl}{4\pi r^2}\sin 2\theta\left[4I_1K_1 - \frac{k_1 r}{2}(I_0K_1 - K_0I_1)\right],$$

$$H_y^{(0)} = \frac{Idl}{2\pi r^2} \times \left\{\sin^2\theta\left[4I_1K_1 - \frac{k_1 r}{2}(I_0K_1 - K_1I_0)\right] - I_1K_1\right\}, \quad (2)$$

$$H_z^{(0)} = \frac{Idl}{2\pi k_1^2 r^4}\sin\theta\left[3 - (3 + 3k_1 r + k_1^2 r^2)e^{-k_1 r}\right],$$

where $\rho_1 = 1/\sigma_1$ is the electrical resistivity of the earth ($\Omega$ m), $\theta$ is the angle in the horizontal plane $xy$ between the axis of HED and the direction to the observation point; $I_n$, $K_n$ are the modified Bessel functions of the first and second kind of order $n$ with argument $k_1 r/2$, respectively.

In the analysis of the structure of the EM field generated by the controlled sources including HED, the near-field, transition, and far-field zones are considered (Zonge and Hughes, 1991).

**The near-field zone** corresponds to the condition $|k_1|r \ll 1$ or $r/d < 0.5$, where $d \cong 503\sqrt{\rho/f}$ is the skin depth. The alternating EM field in the near-field zone behaves as the field of a DC source. In this case, the electrical components of the field depend on the electrical resistivity of the rock and are insensitive to the current frequency. The magnetic components neither depend on the frequency nor on the resistivity of the rock. Therefore, the impedance measurements in the near-field zone are unsuitable for frequency sounding.

In the **transition zone**, the components of the quasi-stationary EM field generated by HED are described by formulas (2). They depend on the frequency of the electric current and the coordinates of the observation point (the $E_y$ component is frequency-independent).

The EM field in the **far-field zone** of HED, where $|k_1|r \gg 1$ or $r/d > 3$–5, has the following components:

$$E_x^{(1)} = \frac{Idl\rho_1}{2\pi r^3}(3\cos^2\theta - 2), \quad E_y^{(1)} = \frac{3Idl\rho_1}{4\pi r^3}\sin 2\theta,$$
$$H_x^{(0)} = \frac{3Idl}{4\pi k_1 r^3}\sin 2\theta,$$
$$H_y^{(0)} = -\frac{Idl}{2\pi k_1 r^3}(3\cos^2\theta - 2), \quad (3)$$
$$H_z^{(0)} = -\frac{3Idl}{2\pi k_1^2 r^4}\sin\theta.$$

The surface impedance components in the far-field zone are described by the following formulas:

$$Z_{xy} = \frac{E_x}{H_y} = -\sqrt{i\rho_1\omega\mu_0} = -\sqrt{\rho_1\omega\mu_0}e^{i\frac{\pi}{4}},$$
$$Z_{yx} = \frac{E_y}{H_x} = \sqrt{i\rho_1\omega\mu_0} = \sqrt{\rho_1\omega\mu_0}e^{i\frac{\pi}{4}}. \quad (4)$$

Taking into account the fact that the moduli of the impedance components are $|Z_{xy}| = |Z_{yx}| = \sqrt{\rho_1\omega\mu_0}$ the resistivity $\rho_1$ can be calculated according to the following formulas:

$$\rho_1 = \frac{1}{\omega\mu_0}|Z_{xy}|^2 = \frac{1}{\omega\mu_0}|Z_{yx}|^2. \quad (5)$$

The impedance phases are calculated from

$$\varphi_Z^{xy} = \varphi_{Ex} - \varphi_{Hy}, \quad \varphi_Z^{yx} = \varphi_{Ey} - \varphi_{Hx}. \quad (6)$$

In the homogeneous half-space and with the time dependence in the form $e^{+i\omega t}$, the impedance phases of $Z_{xy}$ and $Z_{yx}$ in the far-field zone are 45°.

Formulas (4)–(6) illustrate the well-known ideas that the electrical resistivity of the medium and the impedance components $Z_{xy}$ and $Z_{yx}$ in the far-field zone are linked by a simple relationship corresponding to the vertically incident plane wave.

The contour maps of the horizontal electrical and magnetic components of the EM field generated by HED within a quasi-stationary approximation in the first quadrant of the working area are shown in Fig. 1. The calculations are carried out for a model with the electrical resistivity of the earth $\rho_1 = 1000$ Ω m, current frequency $f = 100$ Hz, and $Idl = 100$ A m.

This figure illustrates the structure of the EM field of HED. In the equatorial area of the dipole and on its axis, the amplitudes of the $|E_x|$ and $|H_y|$ components monotonically decrease with distance. The values of $|E_x|$ and $|H_y|$ in the equatorial area are twice as high as the corresponding values on the dipole axis. In the area oriented at an angle of about 35° to the axis of the dipole, $|E_x|$ and $|H_y|$ have significant gradients and linear zones of minimum values. The magnitudes of the $|E_y|$ and $|H_x|$ components monotonically decrease with distance in the area that is oriented at an angle of about 45° to the dipole axis and tend to zero in the equatorial and axial areas. This pattern of behavior of the EM components is also characteristic of the field generated by a cable having a finite length.

According to the structure of the field generated by HED and the cable, the $Z_{xy}$ impedance measurements are used in the segments of the working area, which are located in the equatorial and axial zones of the dipole or the cable. In the area oriented at an angle of about 45° to the dipole or cable, measurements of the $Z_{yx}$ impedance are carried out.

The source in the form of a finite-length cable is used in the CSAMT method. The CSAMT soundings are mainly conducted in the equatorial zone of the cable; they include measurements of the impedance modulus $|Z_{xy}|$ and phase $\varphi_Z^{xy}$, because the $E_x$ and $H_y$ components have higher amplitudes, and the working area (the region of monotonic changes of the EM components) is wider than in the axial zone.

## THE FIELD WITH ALLOWANCE FOR DISPLACEMENT CURRENTS

In the calculations of the components of the EM field in the case of high frequencies, one should use formulas (1) and take into account the displacement currents in the earth and air. If the observation point is located on the surface of the earth ($z = 0$), formulas (1) can be recast. The simplest formula describes the $H_z$ component:

$$H_z^{(0)} = -\frac{Idl}{2\pi}\frac{\sin\theta}{(k_1^2 - k_0^2)r^4} \times \left[(3 + 3k_1 r + k_1^2 r^2)e^{-k_1 r} - (3 + 3k_0 r + k_0^2 r^2)e^{-k_0 r}\right]. \quad (7)$$

It can be seen from this expression that the $H_z$ component depends on the wave number in the earth $k_1 = \sqrt{i\omega\mu_0\sigma_1 - \omega^2\mu_0\varepsilon_1}$, and on the wave number in the air $k_0 = \sqrt{i\omega\mu_0\sigma_0 - \omega^2\mu_0\varepsilon_0}$. At sufficiently high frequencies $f$ and at a sufficiently large distance $r$ from the source to the observation point, the product $k_0 r$ provides a significant contribution in $H_z$ and other components of the EM field.

The fact that the effects of displacement currents in the air should be taken into account for different types of EM sources in the studies that use high frequency signals and solve the problem at a large distance from the source has been noted in a number of previous publications.

Veshev, Ladatko, and Morozova (1983) analyzed the effects caused by the displacement currents in the air and in the ground for the case of a vertical magnetic dipole. They suggested the methods for estimating the electrical resistivity $\rho_1$ and relative permittivity $\varepsilon_1^{rel}$ of the earth from the measurements of two parameters of the EM field, e.g., the ratio between the moduli of two

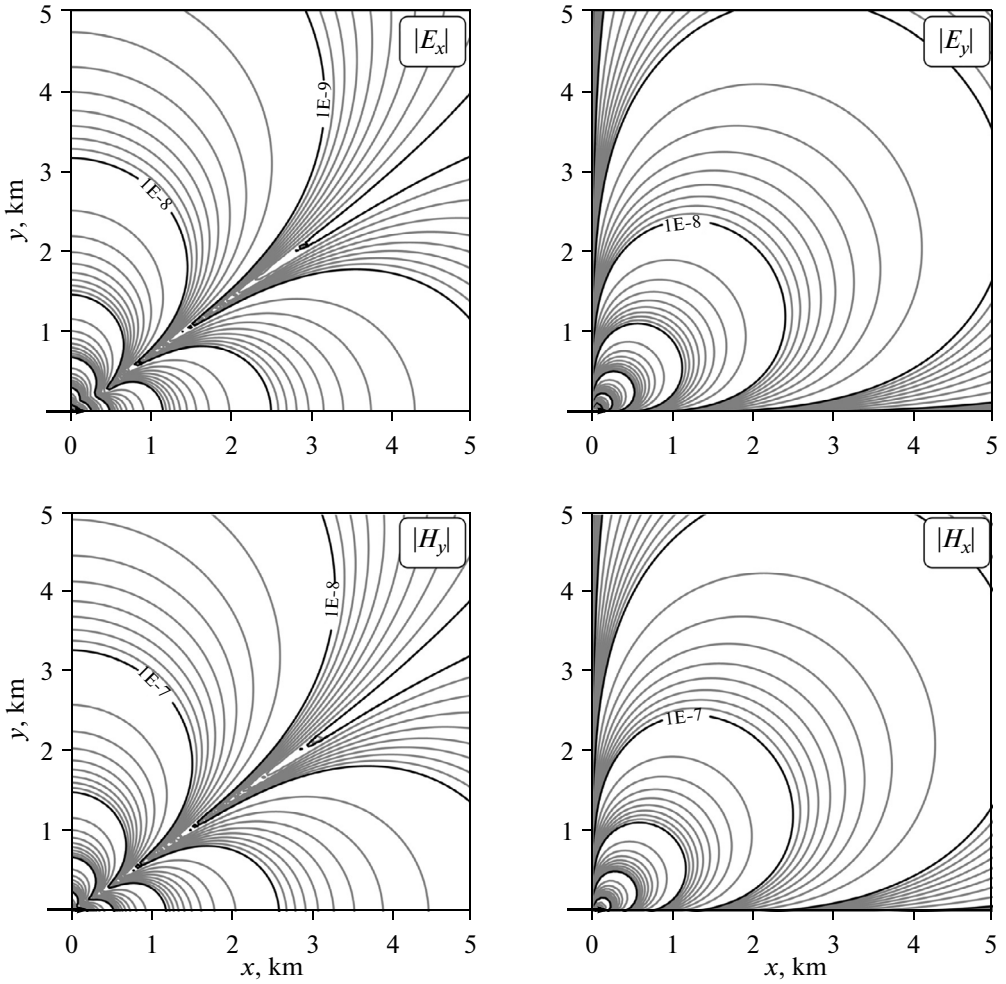


**Fig. 1.** The contour maps of the amplitude of the horizontal electrical ($E_x$, $E_y$, V/m) and magnetic ($H_x$, $H_y$, A/m) field of HED in the quasi-stationary approximation. The dipole is shown by the arrow.

components of the EM field and the phase difference between them.

The boundaries of the quasi-stationary approximation of the electrical field for HED (i.e., the conditions when the displacement currents in the ground and air can be neglected) are assessed in (Egorova and Sapozhnikov, 1983). The estimates are presented as the functions of the parameter $r/\lambda_0$, where $\lambda_0$ is the wavelength of the EM wave in the air, and the parameter $|k_0|r$ for the radial ($E_r$), azimuthal ($E_\varphi$), and vertical ($E_z$) electric field components of HED. According to these authors, the maximal $|k_0|r$, for which the errors associated with neglecting the displacement currents in the air do not exceed 5% in the moduli for different characteristics of the electric field, are estimated at 0.32, 0.22, and 0.37 for $|E_r|$, $|E_\varphi|$, and $|E_z|$, respectively.

The effects of the displacement currents in the air and earth for the horizontal loop source (vertical magnetic dipole) and $H_z$ component in the application to the transient EM method are analyzed in (Spies and Fricshnecht, 1991). In the quoted work, the influence of the displacement currents in the air on the structure of the source EM field is referred to as the "propagation effect". Using the graphs of normalized impedance for the field of vertical magnetic dipole $Z/Z_0$ (or the magnetic number $h_z$ (Kraev, 1965)), one can calculate the limiting values of $|k_0|r$, which are estimated at 1.3 for the modulus of $Z/Z_0$ and 1.2 for the phase.

The displacement currents in the air affect the behavior of the components of the EM field even at relatively low frequencies (a few units to a few dozen Hz) if the distance between the source and the observation point is quite large. As demonstrated by the calculations and observed in the field experiments (Saraev and Kostkin, 1997; 1998), the displacement currents in the air significantly distort the EM field of the Russian high-power ELF transmitter operating at a frequency of 80 Hz at a distance of a few hundred to a few thousand km from the source. Besides, the signals at a large distance (few hundred km) from the transmitter experience a strong impact from the ionosphere, whose lower boundary is located at a height of

60 and 90 km during the daytime and nighttime, respectively.

In the cases of the sources with long-range coverage, it is suggested (Saraev and Kostkin, 1997; 1998; 1999), in addition to the conventional zones (the near-field, transition, and far-field zones) distinguished in the EM field generated by HED and a cable, to consider the **waveguide zone,** where the effects of the ionosphere and displacement currents in the air are significant.

The key features of the waveguide effects arising in the data of the EM studies are analyzed in (Saraev et al., 2011; Saraev and Shlykov, 2012a; 2012b). These effects include the increased amplitudes of the EM components compared to the quasi-stationary field; the change in the directional diagram of the source with the growth in the amplitude of the field along HED and cable; the emergence of elliptical polarization; and the change in the configuration of favorable areas for CSAMT studies. Here, it is noted that in the waveguide zone, the primary field generated by the HED and cable can be approximated by a vertically incident plane wave, and the sounding data can be processed by the methods that are used in the magnetotelluric applications.

In addition to experiencing the influence from the displacement currents in the air, the structure of the HF EM field is also affected by the displacement currents in the earth. The implications of the displacement currents in the air for the results of the RMT method are analyzed in a number of recent publications of T. Kalscheuer (e.g., (Kalscheuer, Pedersen, and Siripunvaraporn, 2008)). Below we consider the effects caused in the normal field of HED by the displacement currents in the air. The displacement currents in the ground are also taken into account in the calculations.

## THE PROCEDURE OF CALCULATIONS

The main difficulty in the calculation of the EM field components by formulas (1) is computing the Hankel transform in the following form

$$\int_0^\infty f(k_0, k_1, m) J_n(mr) dm, \tag{8}$$

where $f(k_0, k_1, m)$ is the function of the parameters of the medium and $J_n(mr)$ is order $n$ Bessel function of the first kind.

In the calculations for quasi-stationary approximation, the most popular method for integrating Bessel functions is the fast Hankel transform (FHT) (Anderson, 1979; Ryzhov, 1989; Guptasarma and Singh, 1997; etc.). This method is applicable if the kernel of integral $f(k_0, k_1, r)$ is a smooth and continuous function, which is fulfilled with $k_0 = 0$.

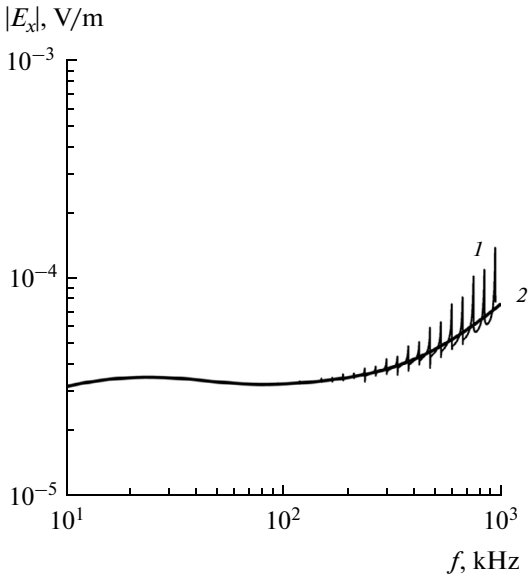


**Fig. 2.** The graph of $|E_x|$ field of HED at $k_0 \neq 0$. (*1*) The results are obtained by the FHT method; (*2*) the results are obtained by the method of partial integration with Wynn's $\epsilon$-extrapolation.

The methods for calculating integral (8) with $k_0 \neq 0$ were considered in (Petrukhin, 2001; Key, 2012; Siemon, 2012). As shown in (Siemon, 2012), the kernel of integral (8) at $k_0 \neq 0$ has a singularity at $m = \omega\sqrt{\mu_0\varepsilon_0}$, which violates the smooth behavior of the integrand.

Figure 2 displays the results of applying the conventional FHT method for calculating $|E_x|$ of HED at $k_0 \neq 0$ with the following parameters of the half-space, source, and coordinates of the observation point: $\rho_1 =$ 1000 Ω m; $\varepsilon_1^{\text{rel}} = 10$, $Idl = 100$ A · m; and $x = 0$, and $y = 1000$ m. The graph of $|E_x|$ has false peaks, which are associated with the specific features of discretization of the set of spatial frequencies $m$. This problem can be solved by different methods. One of them is the special selection of the grid of spatial frequencies $m$ in the way it is done, e.g., in (Siemon, 2012). In this case, adaptation of grid $m$ should be carried out for each frequency $f$.

Another method for the exact integration of Bessel functions implies successive integration on the intervals between the extrema or zeros of $J_n(mr)$:

$$\int_0^\infty f(k_0, k_1, m) J_n(mr)\, dm = \sum_{j=0}^{\infty} \int_{p_j}^{p_{j+1}} f(k_0, k_1, m) J_n(mr)\, dm, \tag{9}$$

where $p_j$ is the spatial frequency $m$ corresponding to the extremum or zero of the Bessel function $J_n(mr)$ with the number $j$. Here, convergence of the series (9)

can be very slow. In order to solve this problem, different extrapolations and transforms are applied. Close attention in (Key, 2012) is attached to the selection of the optimal method among the discussed extrapolation methods in the application to the solution of forward 1D problems of EM sounding within a quasi-stationary approximation. Shanks' transform in the form of the algorithm of $\epsilon$-extrapolation is selected as the simplest and fastest method in (Shanks, 1955; Wynn, 1956).

The results of the calculations quoted in the present paper were obtained by the method of partial integration with $\epsilon$-extrapolation. Integration is carried out between the zeros of the Bessel function by the adaptive Gauss method with seven-point quadratures. If the critical spatial frequency $m_c$ corresponding to the singularity of $f(k_0, k_1, m)$ falls in the interval $[p_j, p_{j+1}]$, where $p_j$ is one of the zeros of the Bessel function, this interval is subdivided into two corresponding subintervals $[p_j, m_c]$ and $[m_c, p_{j+1}]$. The relative accuracy of the calculation of the integrals at each interval is $10^{-9}$, and the relative accuracy of $\epsilon$-extrapolation is $10^{-6}$. As seen in Fig. 2, partial integration with $\epsilon$-extrapolation yields a smooth curve without false maxima.

## THE WAVE ZONE

As mentioned in the previous section, in the case of long-range sources, which are widely used in electromagnetic prospecting, we have suggested distinguishing the waveguide zone, within which the structure of the field is vitally controlled by the influence of the ionosphere and displacement currents in the air. The measurements in the methods of HF electromagnetic prospecting are conducted at a distance of up to a few km from the source, and in these cases, there is no need to take into account the influence of the ionosphere. At the same time, the effects of displacement currents in the air fully express themselves even at a distance of a few hundreds of meters from the source. In these conditions, in addition to considering the fields in the near-field, transition, and far-field zone of the source, which is common practice in the electromagnetic prospecting applications, it is reasonable to also distinguish the **wave zone** of the source, where the structure of the field depends on the displacement currents in the air. The waveguide zone, which has been singled out previously, can be understood as a kind of wave zone.

The wave zone of the different types of sources is typically considered in the problems of radio propagation as the area determined by the criterion $r \gg \lambda_0$, where $r$ is the distance from the source and $\lambda_0$ is the wavelength of the EM wave in vacuum (Feinberg, 1999). Previously, the wave zone in the radio physical sense has not been considered in the EM prospecting applications, and the behavior of the EM field components in this zone has not been analyzed in detail except for the quoted studies, which present the estimates on the size of the zone of the quasi-stationary approximation.

Let us now analyze the criterion for separating the wave zone, which takes into account the parameters of the source and the distance to the observation point. We only consider the electrical components of the EM field since the magnetic field behaves similarly. We delineate the zone where the displacement currents in the air do not exert a significant impact on the EM field of HED (the quasi-stationary zone). For doing this, we use the parameter $\Delta|E|$, which characterizes the changes in the electrical field in the wave zone with respect to the quasi-stationary approximation:

$$\Delta|E| = 100\% \times \frac{\left|E^{k_0 \neq 0}\right| - \left|E^{k_0 = 0}\right|}{\left|E^{k_0 \neq 0}\right|}. \qquad (10)$$

Figure 3 displays the contour maps of the parameters $\Delta|E_x|$ and $\Delta|E_y|$ calculated for HED located on the surface of the half-space with $\rho_1 = 1000\ \Omega$ m, $\varepsilon_1^{\text{rel}} = 10$ at $f = 100$ kHz. The dipole (shown by the arrow) is located at the origin of the coordinates and oriented along the $x$ axis. In this case, in the analysis of the influence of the displacement currents in the air, the calculations also take into account the effects of the displacement currents in the ground that appear at these frequencies.

We delineate the region of the quasi-stationary approximation as the area where $\Delta|E|$ does not exceed the limiting value of 5%. In the case of the $E_x$ component in the equatorial and axial zones of the dipole, the boundary is drawn by the limiting values $|k_0|y = 0.33$ (which corresponds to the distance $y = 160$ m for the selected parameters of the medium and the source) and $|k_0|x = 1.0$ ($x = 480$ m), respectively. In the area oriented at an angle of about 35° to the direction of the dipole, the isolines of $\Delta|E_x|$ show complicated behavior, which is not related to the position of the boundary between the quasi-stationary and wave zone but is due to the misalignment of the minima in $|E_x|$ in the cases considered.

The boundary of the quasi-stationary approximation for the $E_y$-component follows the line $|k_0|r = 0.45$ ($r = 200$ m). Generally, the estimates of the boundary of the quasi-stationary approximation closely agree with the results of the previous studies discussed above.

When the quasi-stationary approximation is used in the practice of EM prospecting, the near-field, transition, and far-field zones for different types of sources are typically distinguished with reference to the skin depth $d$ of the field, which depends on the frequency and resistivity of the earth. The position of the boundary between the quasi-stationary and wave zones is insensitive to the resistivity of the rocks and skin depth of the field. Comparing the positions of the boundary between the quasi-stationary and wave zones (specified by criterion (10)) at different frequen-

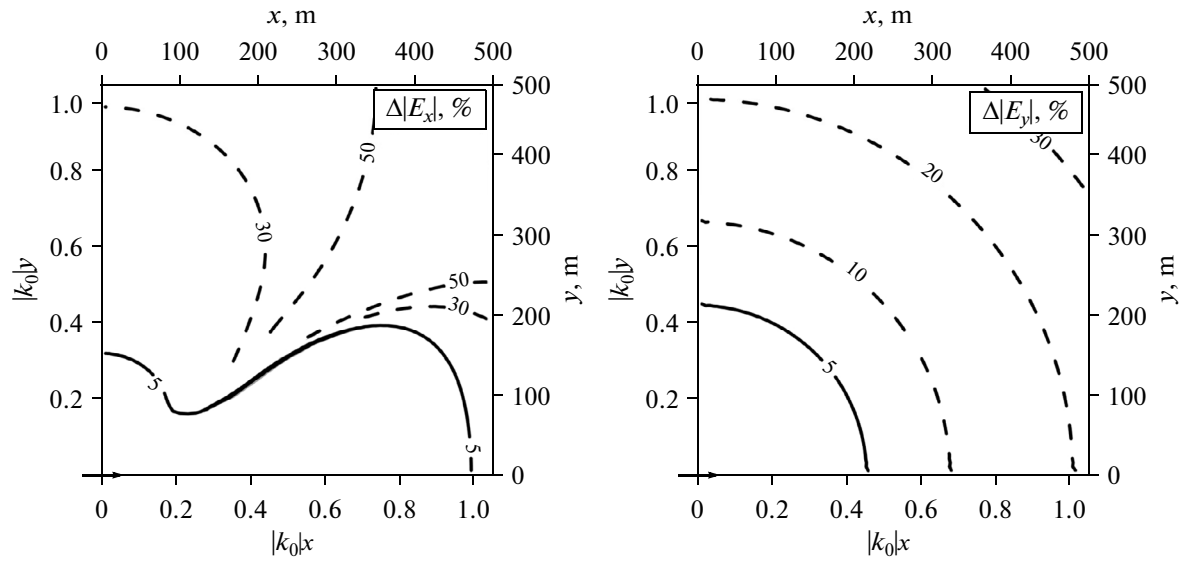


**Fig. 3.** The boundaries of quasi-stationary zone (the solid lines) for the $E_x$ and $E_y$ components of HED for $f = 100$ kHz and the parameters of the earth $\rho_1 = 1000\ \Omega$ m and $\varepsilon_1^{rel} = 10$.

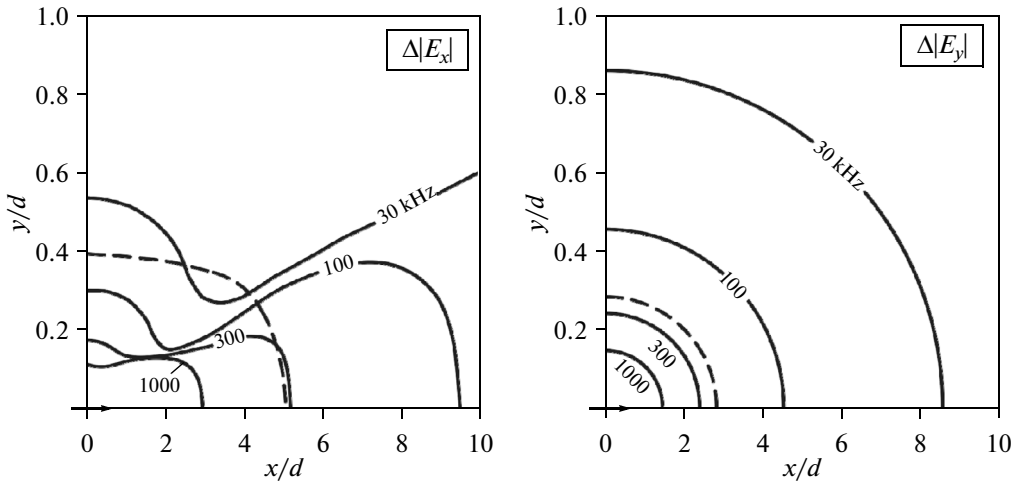


**Fig. 4.** The boundaries of the quasi-stationary zone of HED for $E_x$ and $E_y$ with different frequencies of the dipole current ($\rho_1 = 1000\ \Omega \cdot$ m, $\varepsilon_1^{rel} = 10$). The dashed line corresponds to the boundaries between the transition and far-field zones within the quasi-stationary approximation.

cies with the position of the boundary between the transition and far-field zones (drawn according to the skin depth), we see that, depending on frequency, the first boundary can be located both farther from and nearer to the source than the second boundary (Fig. 4). The corresponding limiting distances with different normalization are presented in the table.

We note that if the boundary between quasi-stationary and wave zone is located closer to the source than the boundary between the transition and far-field zones, the behavior of the EM field in the considered far-field zone will differ from the common regularities of the far-field zone. As demonstrated below, considering the displacement currents in the air, the far-field zone will be prone to wave effects; however, at the same time, the source field in this zone still admits its approximation by the vertically incident plane wave.

There are several effects manifesting themselves in the wave zone that should be taken into account in the studies by the HF sounding methods. The maps of iso-

The position of the boundary between the quasi-stationary and wave zone for different frequencies

| $f$, kHz | Parameter of the distance | $\|E_x\|$ | | $\|E_y\|$ |
|---|---|---|---|---|
| | | equator | axis | |
| 30 | $r$, m | 520 | 1600 | 700 |
| | $r/d$ | 6 | 17 | 8 |
| 100 | $r$, m | 160 | 480 | 200 |
| | $r/d$ | 3 | 10 | 4 |
| 300 | $r$, m | 50 | 160 | 70 |
| | $r/d$ | 2 | 6 | 3 |
| 1000 | $r$, m | 15 | 50 | 20 |
| | $r/d$ | 1.0 | 3.0 | 1.5 |

lines of $|E_x|$ and $|E_y|$ calculated with allowance for the displacement currents are shown in Fig. 5. By comparing the contour maps of $|E_x|$ in the quasi-stationary zone (Fig. 1) and wave zone (Fig. 5), we see that the configuration of the minimum of the field, which is oriented at an angle of about 35° to the dipole axis, is changed in the wave zone. This minimum becomes smoother and shifts towards the equatorial area of the dipole. The configuration of the isolines of $|E_y|$ also changes: in the wave zone, the isolines are stretched at an angle of 45° to the dipole.

Consider in more detail the attenuation of the electrical field of HED as a function of distance. Within the quasi-stationary approximation, the following regularities are observed in the near-field, transition, and far-field zones. In the near-field zone, the horizontal electric field $E_x$ and magnetic field $H_y$ decay as $1/r^3$ and $1/r^2$, respectively. In the transition zone, the decay rate of $E_x$ and $H_y$ mainly varies from $1/r^2$ to $1/r^3$ (up to $1/r^4$ on the axis of the dipole for $E_x$), depending on the particular component of the field, orientation of the profile, and the distance to the source. In the far-field zone, $E_x$ and $H_y$ decay at $1/r^3$ (Zonge and Hughes, 1991). The different decay rates of $E_x$ and $H_y$ in different zones are illustrated by Fig. 6. The boundary between the transition and far-field zones for the equatorial area of the dipole is drawn in this case by the condition $y/d = 4$ with $f = 100$ kHz and $\rho_1 = 1000\ \Omega$ m.

When analyzing the decay of the source field in the far-field zone (outside the region of the quasi-stationary approximation), if the wave zone is located farther than the boundary between the transition and far-field zones, one observes different decay rates in the equatorial area of the dipole and on its axis. In the equatorial area of HED, the $E_x$ and $H_y$ fields decay as $1/r^2$, while the decay rate on the axis is $1/r$ (Fig. 6).

The change in the directional diagram of HED is a characteristic feature of the wave zone (Fig. 7). In the case of the quasi-stationary field in the far-field zone of the source, the amplitude of the $E_x$ component in the equatorial area is double the corresponding value on the dipole axis (Fig. 7a), whereas in the wave zone, the amplitude of the $E_x$ field on the axis of the dipole is significantly higher than in its equatorial area (Fig. 7c). Figure 7b shows an intermediate shape of the directional diagram. This feature of the directional diagram of HED located on the surface of the Earth is well known in radio physics (Kontorovich, 1956); however, it has not been previously taken into account in EM prospecting.

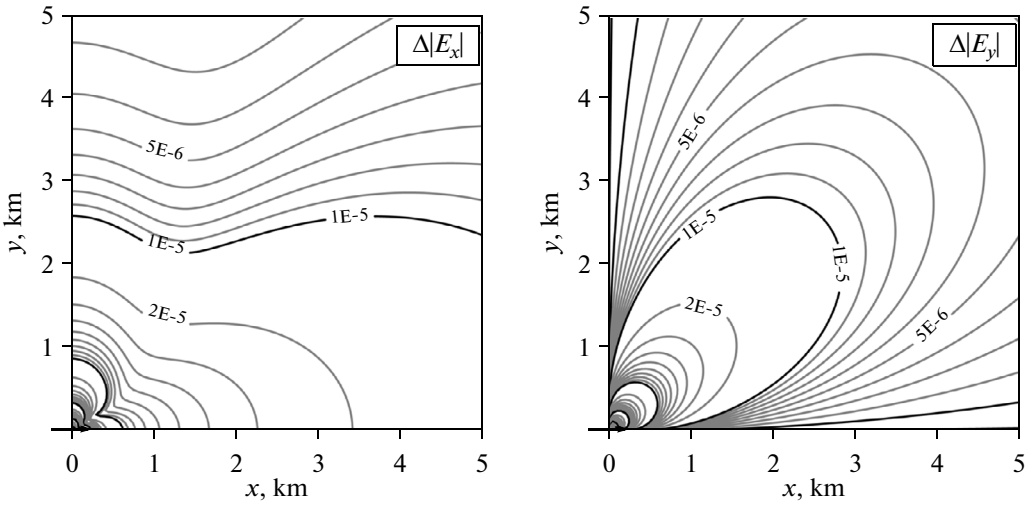


**Fig. 5.** The contour maps of the horizontal electrical field of HED in the wave zone. $|E_x|$ and $|E_y|$ are expressed in V/m; $\rho_1 = 1000\ \Omega \cdot$ m, $\varepsilon_1^{rel} = 10$; $f = 100$ kHz.

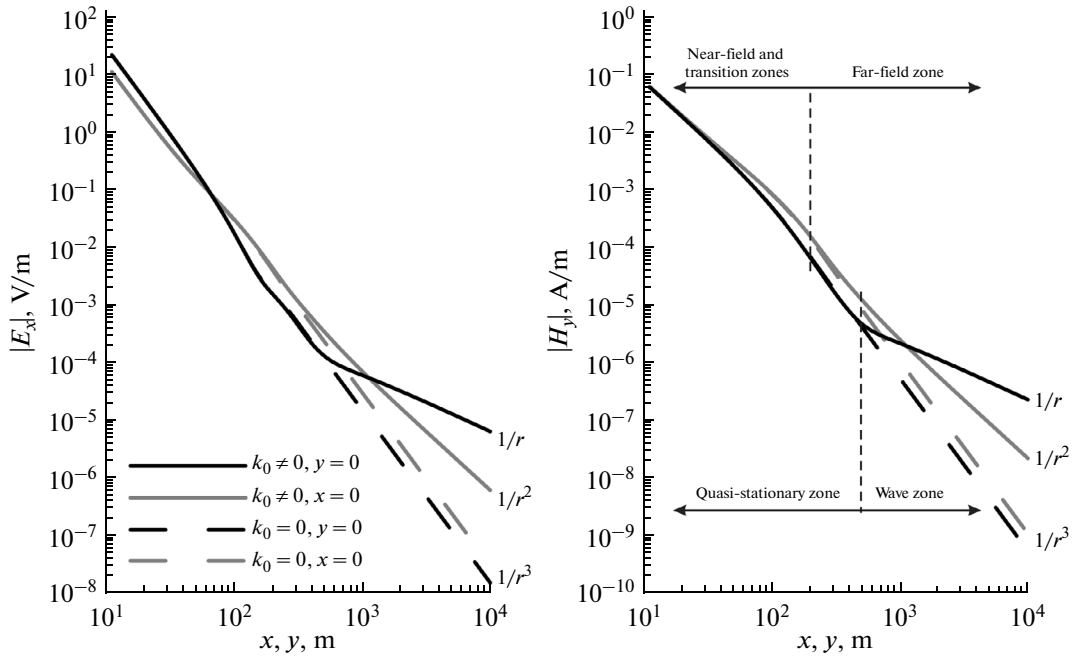


**Fig. 6.** The dependences of $|E_x|$ and $|H_y|$ of HED as the functions of distance on the axis of the dipole ($y = 0$) and in its equatorial area ($x = 0$). The solid and dashed lines correspond to $k_0 \neq 0$ and $k_0 = 0$, respectively.

The configurations of the contour maps (Figs. 1 and 5) and directional diagram (Fig. 7) show that the wave zone of HED is marked by the narrowing of the favorable interval for $Z_{xy}$ impedance measurements in the equatorial area of the dipole and widening of this interval in the direction along the dipole. As is known, the main working area in the CSAMT method lies in the equatorial area of the source. In the high-frequency applications, the working area should be selected with allowance for the behavior of the field in the wave zone.

We note that the configuration of the favorable areas for $Z_{xy}$ impedance measurements changes with increasing frequency. At low frequencies (from a few kHz to a few dozen kHz), the favorable interval is located in the equatorial area of the dipole, while at a higher frequency, it falls in its axial neighborhood. At the same time, as it will be demonstrated below, the horizontal components of the EM field rather have elliptical polarization, and $Z_{xy}$ impedance measurements can be carried out in any part of the working area near the source.

When selecting the position of the working area, one should also take into account the fact that the measurements of the controlled-source signals are more reliable at low frequencies and that they are carried out farther from the source than measurements of HF signals. Therefore, it is preferable to carry out the survey in the axial part of the source.

As is known, within the quasi-stationary approximation, the electrical and magnetic fields of HED are linearly polarized. Under the influence of the displacement currents in the air, the polarization becomes elliptical at a certain distance from the source (Saraev and Kostkin, 1998). We calculated the parameters of the polarization ellipses of the electric field (major axis $a$, minor axis $b$, and the angle of horizontal rotation of the major axis) for $f = 300$ kHz and $\rho_1 = 1000\ \Omega$ m (Fig. 8). For a clearer illustration, the semiaxes $a$ and $b$ at each point are normalized by the major semiaxis ($a = 1$, $b = b/a$).

It is seen in Fig. 8 that electrical field $E$ is linearly polarized in the horizontal plane in the wave zone on the axis of the dipole. In the area oriented at an angle of about 35° to the dipole axis, the polarization is maximally elliptical ($b/a \to 1$). In this case, the area of an elliptically polarized field is quite wide at the selected frequency. Besides elliptical polarization, we also observe a certain delay of the turn of the ellipses relative to the direction of linear polarization for the quasi-stationary approximation.

The area where the polarization of the field is maximally elliptical near the dipole coincides with the area of the minimal $E_x$, which is oriented at an angle of about 35° to the dipole. With the increase in the distance to the source or with the increase in frequency, this area is shifted towards the equator of the dipole (Figs. 8 and 9). The presence of ellipticity makes it possible to implement tensor impedance soundings with a single source of the EM field.

In the wave zone, the possibility of plane-wave approximation of the HED field persists, together with the possibility to use formulas (4)–(6) for calculating the apparent resistivities and impedance phases and

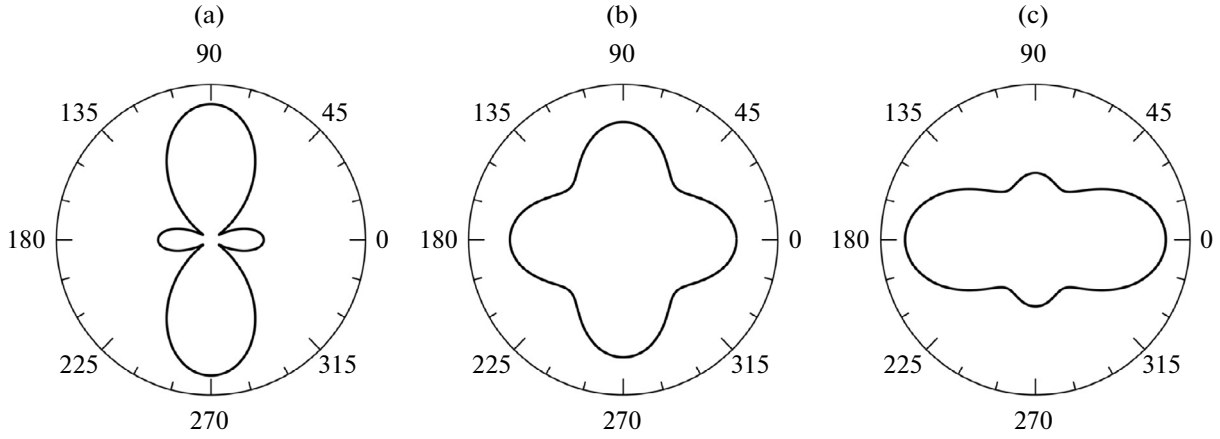


**Fig. 7.** The directional diagram of HED for $|E_x|$ at a distance of (a) 300 m, (b) 1100 m, and (c) 2000 m from the source at $f =$ 100 kHz and $\rho_1 = 1000\ \Omega$ m. The values of $|E_x|$ are normalized to the corresponding maximal values for each case.

their subsequent inversion by the methods and programs of magnetotelluric inversion (Fig. 10). Under the influence of the displacement currents in the air, the amplitudes of the electrical and magnetic fields increase compared to the quasi-stationary approximation (Fig. 10a); however, their proportion remains constant and the apparent resistivity and impedance phase curves do not change (Fig. 10b).

Thus, the following effects are observed in the wave zone of HED:

—the amplitudes of the $E$ and $H$ fields in the wave zone decay lower than in the quasi-stationary zone; their decay rates are proportional to $1/r^2$ and $1/r$ in the equatorial and axial area of the dipole, respectively;

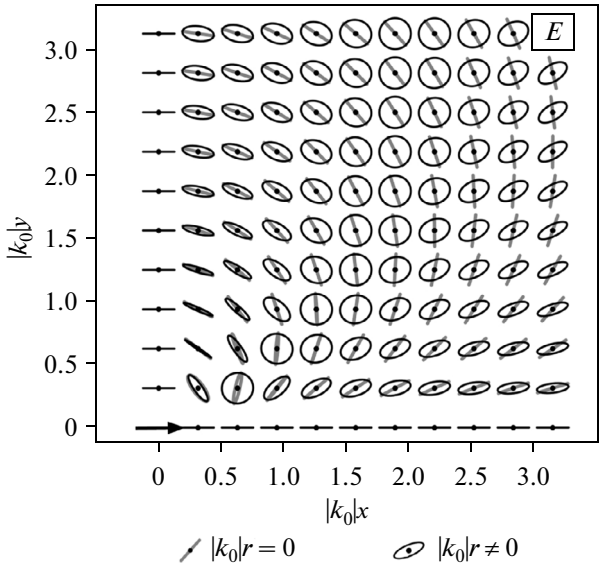


**Fig. 8.** The polarization ellipses of the electric field of HED for $f =$ 300 kHz.

—the directional diagram of the source is changed in the wave zone, and the maximum radiation is observed along the axis of the dipole. Here, the amplitude of $E_x$ in the quasi-stationary zone of the source is by a factor of two higher than in the axial area, and the amplitude of $E_x$ on the axis of the dipole in the wave zone is severalfold higher;

—the location of the working areas is changed in the wave zone and the most favorable working area for $Z_{xy}$ impedance measurements is located in the axial part of the dipole;

—the characteristic feature of the EM field of HED in the wave zone is elliptical polarization of the $E$ and $H$ in the horizontal plane; here, the areas of elliptical polarization coincide with the areas of the minima in the directional diagrams of horizontal distributions of $E$ and $H$;

—the azimuths of major axes of horizontal polarization ellipses of $E$ and $H$ are delayed relative to the directions of the linear polarization for the quasi-stationary approximation.

## THE RESULTS OF EXPERIMENTS

The field experiments were conducted with the use of CSRMT instrumentation and software designed for the controlled-source radio magnetotelluric sounding. This complex includes RMT-F recorder (Tezkan and Saraev, 2008) and GTS-1 transmitter (Simakov et al., 2010; Saraev et al., 2011). The RMT-F recorder has five synchronous recording channels (two electrical channels for recording $E_x$ and $E_y$ and three magnetic channels for recording $H_x$, $H_y$, and $H_z$), which make it possible to measure the total tensor of surface impedance and magnetic transfer functions (tipper). The entire frequency range of the recorder (1–1000 kHz) is subdivided into three subintervals: 1–10 kHz with a sampling frequency of 39 kHz, 10–100 kHz

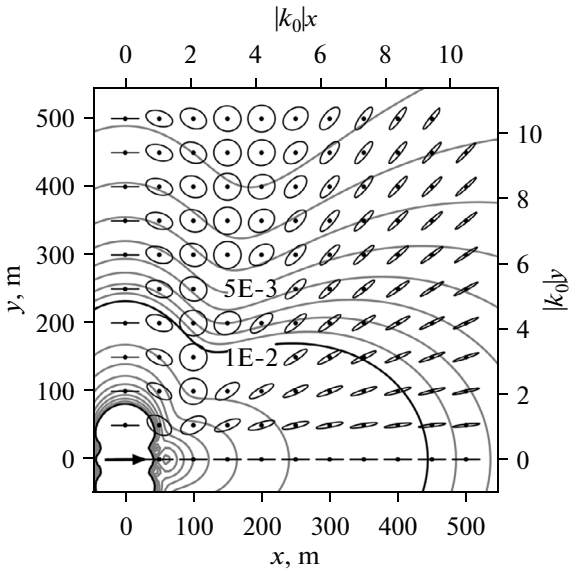


**Fig. 9.** The polarization ellipses of the electric field of HED for $f = 1$ MHz shown together with the isolines of $|E_x|$.

(312 kHz), and 100–1000 kHz (2496 kHz). The GTS-1 transmitter operates in the frequency band of 0.1 Hz to 1 MHz and provides the maximal output voltage of 288 V and maximal power of 1 kW. The GTS-1 transmitter is fed by a standard 3-kW gasoline engine with an output frequency of 50 Hz.

The measurements were conducted in the Kingisepp region of Leningrad oblast. The geological section in the studied area is dominated by sand and loam. The upper layers (to a depth of 10–12 m) are mainly composed of sands with resistivity $\rho = 400$–$1000\ \Omega$ m. The lower horizons are loam with $\rho = 100$–$200\ \Omega$ m. The results of DC profiling with a symmetric Wenner array of a electrode with spacing AB = 10 and 30 m along the CSRMT profile indicate that the geoelectrical section is highly heterogeneous on the flanks of the profile.

In the CSRMT measurements, the GPSMP cable $1 \times 4.0$ with a length of 400 m was used as the transmitting antenna. The basic frequencies were set at 1.05, 10.5, and 105 kHz. The current in the transmitter circuit was 3.2, 2.4, and 0.8 A, respectively.

The measurement points were arranged along the profile parallel to the transmitting antenna in its equatorial area (Fig. 11b). The distance between the source and receiver was 1.8–2 km. At each station, measurements with the induction magnetic antennas and ungrounded electric lines with a length of 20 m were successively carried out in the three frequency bands of 1–10 kHz, 10–100 kHz, and 100–1000 kHz. Recording in the time-series mode and the absence of frequency selectivity in the LC circuit of the transmitter antenna made it possible to simultaneously measure the base transmitter frequency and its 3rd, 5th, 7th, and 9th odd harmonics.

The polarization ellipses of the recorded and calculated $E$ field in the horizontal plane are shown in Fig. 11a. The calculations were carried out for the model of a homogeneous half-space with a resistivity of 250 Ω m. At frequencies of 30–50 kHz, the linear polarization is changed into elliptical polarization. In the equatorial area of HED, the polarization ellipses are predominantly oriented along the moment of the source (the AB line). Probably, due to

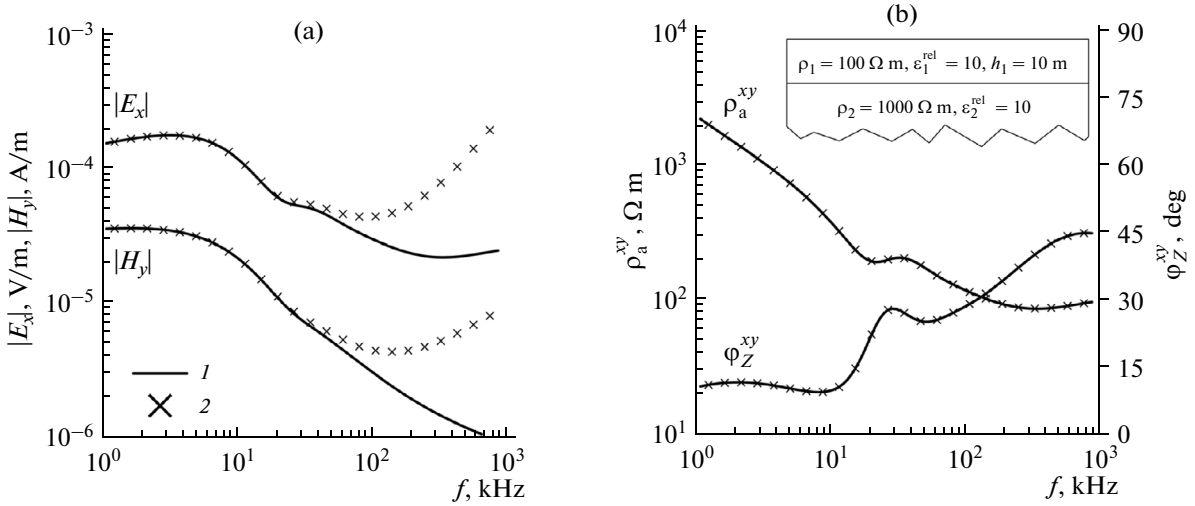


**Fig. 10.** The graphs of apparent resistivity $\rho_a^{xy}$, impedance phases $\varphi_Z^{xy}$, and moduli of the $|E_x|$ and $|H_y|$ fields for HED above two-layer medium. *1* and *2* correspond to $k_0 = 0$ and $k_0 \neq 0$, respectively. The observation point is located at $x = 0$ m and $y = 500$.

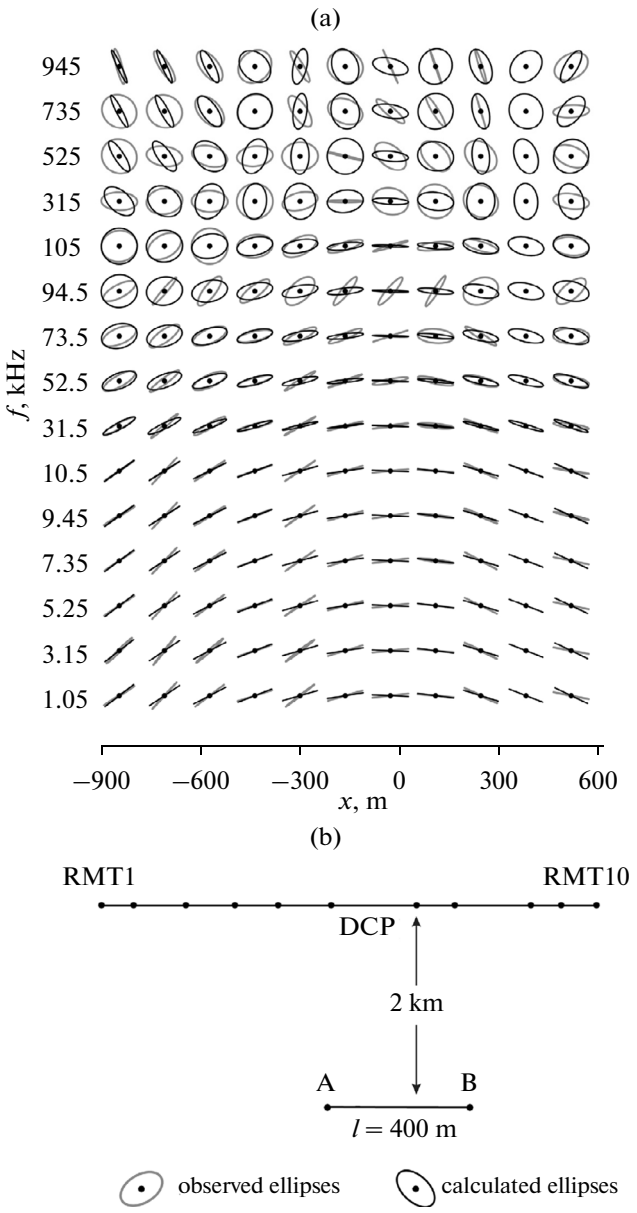


**Fig. 11.** (a) The observed and calculated polarization ellipses of the electrical field $E$ along the CSRMT profile (horizontal axis). The vertical axis shows the frequencies of measurements on the profile. (b) The sketch of the measurements (arbitrary scale). AB is the transmitting antenna; RMT1–RMT10 are the CSRMT sounding points; and DCP is the line of DC electrical profiling with a symmetrical array.

the local heterogeneities in the upper layers of the earth, which affected the data of DC electrical profiling, the ellipses of the observed fields differ from their model predictions. At the same time, reasonable agreement between the measurements and calculations is observed in quite a large spatial–frequency domain.

## CONCLUSIONS

In this paper, we consider the specific features of the EM field generated by HF horizontal electric dipole. In the frequency range from dozens to hundreds of kHz, quite far (within a few hundreds of meters to a few kilometers) from the observation point, the conditions of a quasi-stationary approximation are not satisfied, and it is necessary to take into account the displacement currents in the air. In this situation, in addition to the near-zone, transition, and far-field zones of the controlled source, which are usually distinguished in the common practice of electromagnetic prospecting, it is also reasonable to introduce the wave zone of the source, in which the behavior of the components of the EM field has a few specific features. The wave zones of the different types of sources are traditionally considered in the problems of radiowave propagation; however, in the case of electromagnetic soundings, only the size of the zone of the quasi-stationary approximation was previously assessed.

In order to calculate the components of the normal field of HED, we developed the program that takes into account the displacement currents in the ground and air. Using the method of partial integration with $\epsilon$-extrapolation, we carried out highly accurate calculations of the integrals (within semi-infinite limits) of the functions that have a singularity in the case of a nonzero wave number in the air.

Based on the calculations, we have analyzed the specificity of delineating the wave zone of HED. The location of the boundary between the quasi-stationary zone and wave zone does not depend on the electrical properties of the conductive half-space. It is also insensitive to the position of the boundary between the transition and far-field zones, which are typically delineated according to the criterion of the skin depth of the field. For the $E_x$ and $H_y$ components, the boundary between the quasi-stationary and wave zones on the axis of the dipole corresponds to the numerical distance $|k_0|r = 1.0$; and in the equatorial area of the dipole, this boundary corresponds to $|k_0|r = 0.33$. In the case of $E_y$ and $H_x$, this boundary corresponds to $|k_0|r = 0.45$. These limiting values of the numerical distance $|k_0|r$ for the frequency of 100 kHz correspond to distances of 480, 160, and 200 m.

Based on the calculations, we have analyzed the pattern of the EM field of HED in the wave zone, where the following wave effects have been determined:

—the amplitudes of the electric and magnetic fields decay more slowly than in the quasi-stationary approximation;

—the directional diagram of the source is changed in the wave zone: the maximum radiation is observed on the axis of the dipole;

—the configuration of the working area is changed in the wave zone: the most favorable area is located in the axial zone of the source;

—the electrical and magnetic fields become elliptically polarized;

—the major axes of the polarization ellipses are turned relative to the direction of linear polarization of the quasi-stationary field.

The amplitude and phase of the EM field impedance in the wave zone coincide with the impedance of quasi-stationary field, which makes it possible to apply the methods and software tools of magnetotellurics, which are developed for the plane wave model, in the inversion of the sounding curves.

The elliptical polarization of the EM field of HED arising in the wave zone opens the possibility to carry out tensor measurements using a single source of the field. The presence of elliptical polarization is demonstrated by the field experiments.

## ACKNOWLEDGMENTS

The work was supported by the research grant from the St. Petersburg State University and the "Geomodel" center of the university.

## REFERENCES

Anderson, W.L., Numerical integration of related Hankel transforms of orders 0 and 1 by adaptive digital filtering, *Geophysics*, 1979, vol. 44, pp. 1287–1305.

Bastani, M., EnviroMT—A new controlled source/radio magnetotelluric system, *Acta Universitatis Upsaliensis*, 2001, p. 179.

Egorova, L.V. and Sapozhnikov, B.G., Estimating the limits of quasi-stationary approximation for low-frequency normal electrical field, in *Metody razvedochnoi geofiziki* (Methods for Exploration Geophysics), St. Petersburg: NPO Rudgeofizika, 1983, pp. 85–97.

Feinberg, E.L., *Rasprostranenie radiovoln vdol' zemnoi poverkhnosti* (Radio Wave Propagation along the Earth's Surface), 2nd ed., Moscow: Nauka, 1999.

Fock, V., Zur berechnung des electromagnetischen wechselstromfelds bei ebener begrenzung, *Ann. Physik*, 1933, vol. 17, no. 4.

Guptasarma, D. and Singh, B., New digital linear filters for Hankel $J(0)$ and $J(1)$ transforms, *Geophys. Prospect.*, 1997, vol. 45, pp. 745–762.

Kalscheuer, T., Pedersen, L.B., and Siripunvaraporn, W., Radiomagnetotelluric two-dimension forward and inverse modeling accounting for displacement currents, *Geophys. J. Int.*, 2008, vol. 175, pp. 486–514.

Key, K., Is the fast Hankel transform faster than quadrature?, *Geophysics*, 2012, vol. 77, pp. F21–F30.

Kontorovich, M.I., *Antennye ustroistva* (Antenna Means), Leningrad: Voennaya akademiya svyazi, 1956.

Kraev, A.P., *Osnovy geoelektriki* (Basics of Geoelectrics), 2nd ed., Leningrad: Nedra, 1965.

Petrukhin, B.P., *Osobennosti rascheta krivykh vysokochastotnykh elektromagnitnykh zondirovanii* (Peculiarities in the Calculation of High-Frequency Electromagnetic Sounding Curves), Available from VINITI, 2001, no. 1490B_01.

Ryzhov, A.A., Algorithm for calculating electromagnetic fields in polarized horizontally layered media, *Izv. Akad. Nauk SSSR, Fiz. Zemli*, 1989, no. 2.

Saraev, A. and Kostkin, P., Structure of ELF radio station electromagnetic field, in *Russian-German Seminar "Actual Problems in Deep EM Studies,"* Moscow, 1997.

Saraev, A.K. and Kostkin, P.M., Structure of electromagnetic field of ELF radio transmitter, *Vopr. Geofiz.*, 1998, no. 35, pp. 117–135.

Saraev, A. and Kostkin, P., Waveguide effects in the ELF radio stations electromagnetic field, *RIO'99 International Congress*, Rio de Janeiro, Brazil, 1999.

Saraev, A.K., Denisov, R.V., Shlykov, A.A., Golovenko, V.B., Larionov, K.A., Vasil'ev, A.V., Vladimirov, D.N., and Astakhova, N.L., Specifics of CSAMT soundings with high-power source, in *Pyataya vserossiiskaya shkola-seminar imeni M.N. Berdichevskogo i L.L. Vanyana po elektromagnitnym zondirovaniyam Zemli* (5th All-Russian Berdichevsky and Vanyan Workshop on Electromagnetic Soundings of the Earth), St. Petersburg, 2011, pp. 307–310.

Saraev, A.K., Simakov, A.E., and Tezkan, B., Foot, mobile and controlled source modifications of the radiomagnetotelluric method, *Near Surface 2011: 17th European Meeting of Environmental and Engineering Geophysics*, Leicester, UK, 2011.

Saraev, A. and Shlykov, A., CSAMT with the long-range action of thousands kilometers, *74th EAGE Conf. and Exhibition Incorporating SPE EUROPEC 2012a*, Copenhagen, Denmark, 2012a, p. 266.

Saraev, A. and Shlykov, A., Electromagnetic field features of the CSAMT with the long-range action of thousands kilometers, *Extended Abstract, 21st EM Induction Workshop*, Darwin, Australia, 2012b, S1_P18.

Shanks, D., Nonlinear transformations of divergent and slowly convergent sequences, *J. Math. Phys.*, 1955, vol. 34, pp. 1–42.

Siemon, B., Accurate 1D forward and inverse modeling of high-frequency helicopter-borne electromagnetic data, *Geophysics*, 2012, vol. 77, WB71–WB87.

Simakov, A., Saraev, A., Antonov, N., Shlykov, A., and Tezkan, B., Mobile and controlled source modifications of the radiomagnetotelluric method and prospects of their application in the near-surface geophysics, *20th Workshop on Electromagnetic Induction in the Earth*, Giza, Egypt, 2010, S5–P9.

Song, Y., Kim, H.J., and Lee, K.H., High-frequency electromagnetic method for subsurface imaging, *Geophysics*, 2002, vol. 67, pp. 501–510.

Spies, B.R. and Frischknecht, F.C., Electromagnetic sounding, in *Electromagnetic Methods in Applied Geophysics*, Tulsa: SEG, 1991, pp. 285–425.

Stefanescu, S.S., Das electromagnetishe normalfild der waagerechten nilderfrequenz-dipols, *Beitr. Angew. Geophysik*, 1942, vol. 9, nos. 3/4. *Gerlands Beitr. Geophysik*, 1950, vol. 61, no. 3.

Strangway, D.W., Swift, C.M., and Holmer, R.C., The application of audio-frequency magnetotelluric (AMT) to mineral exploration, *Geophysics*, 1973, vol. 38, pp. 1159–1175.

Tezkan, B. and Saraev, A., A new broadband radiomagnetotelluric instrument: Application to near surface investigations, *Near Surf. Geophys.*, 2008, vol. 6, no. 4, pp. 245–252.

Vanyan, L.L., *Elektromagnitnye zondirovaniya* (Electromagnetic Sounding), Moscow: Nauchnyi mir, 1997.

Veshev, A.V., *Elektroprofilirovanie na postoyannom i peremennom toke* (DC and AC Electric Resistivity Profiling), 2nd ed., Leningrad: Nedra, 1980.

Veshev, A.V., Ladatko, O.N., and Morozova, O.M., Normal field of vertical magnetic dipole, *Vopr. Geofiz.*, 1983, vol. 30, pp. 159–204.

Ward, S.H. and Hohmann, G.W., Electromagnetic theory for geophysical applications, in *Electromagnetic Methods in Applied Geophysics*, Tulsa: SEG, 1987, pp. 131–312.

Wynn, P., On a device for computing the $e_m(S_n)$ transformation, *Math. Tables Other Aids Comput.*, 1956, no. 54, pp. 91–96.

Zaborovskii, A.I., *Peremennye elektromagnitnye polya v elektrorazvedke* (Alternating Electromagnetic Fields in Geophysics), Moscow, 1960.

Zonge, K.L. and Hughes, L.J., Controlled source audiofrequency magnetotellurics, in *Electromagnetic Methods in Applied Geophysics*, Tulsa: SEG, 1991, pp. 713–809.

*Translated by M. Nazarenko*